Progress In Electromagnetics Research, PIER 29, 169–185, 2000

PULSE SIGNAL SCATTERING FROM PERFECTLY CONDUCTING COMPLEX OBJECT LOCATED NEAR UNIFORM HALF-SPACE

O. I. Sukharevsky, S. A. Gorelyshev, V. A. Vasilets, and A. V. Muzychenko

Institute of Radiophysics and Electronics NAS of Ukraine
Kharkiv Military University
P.O. Box 4677, Kharkiv 310022, Ukraine

Abstract–The approximative calculation technique of the pulse signal backscattering for the perfectly conducting electrically large object (with small curvatures) located near the boundary of the uniform half-space (perhaps, with the complex parameters) is proposed. The calculation results of electromagnetic fields scattered from perfectly conducting sphere and complex shape objects located near the ground surface are demonstrated and discussed.

1. INTRODUCTION

This paper presents an approximate method for calculation of pulse signal backscattering from perfectly conducting electrically large objects (with small curvatures) located near the boundary of uniform half-space (with both real and complex electrical parameters). Results of this method may be used for obtaining a priori information about scattering characteristics of ground objects in radar detection and recognition.

The method is based on field integral representations obtained from Lorenz's lemma. These representations account for electromagnetic interactions between a perfectly conducting scatterer and uniform half-space boundary. Then, we obtained high-frequency approximation of transient characteristic of the object (for backscattering in far field zone). This approximation is obtained accounting for influence of material half-space boundary. Further, by a transient or impulse characteristics we mean their asymptotics near the wave front. It is well known that such asymptotics are in correspondence with short-wave asymptotics in frequency domain. Transient characteristic allows to obtain the object response to arbitrary shaped plane pulse wave.

In the general case, the calculation of pulse response of perfectly conducting object, which is located near ground surface is reduced to determination of summary field scattered by the object when it is in free space and for different directions of sounding pulse incidence.

The method for calculation of pulse characteristics of smooth perfectly conducting objects in bistatic case, based on physical optics approximation [4], has been proposed in [1].

2. FORMULATION OF THE PROBLEM AND THE MAIN CALCULATION RELATIONS

Consider a perfectly conducting object located near the ground surface. In order to calculate the electromagnetic field scattered by the object it is necessary to take into account mutual interaction in the system "object-half-space with ground parameters". For this purpose one can obtain the integral representations of the fields scattered by such system.

We consider a plane pulse wave (signal):

$$\begin{aligned} \vec{E}^0\left(\vec{R}^0, t\right) &= \vec{p}^{\,0} Q(t), \\ \vec{H}^0\left(\vec{R}^0, t\right) &= \sqrt{\frac{\varepsilon_0}{\mu_0}}\left[\vec{p}^{\,0} \times \vec{R}^0\right] Q(t), \end{aligned} \tag{1}$$

obliquely incident on perfectly conducting object with surface $\boldsymbol{S}$ located above the boundary $\boldsymbol{L}$ of the dielectric half-space V^+ (Fig. 1). Here $Q(t)$ is a function that describes temporary dependence of the signal, $\vec{R}^0 = (-\sin\theta, 0, -\cos\theta)$; $\vec{p}^{\,0} = (p_1, p_2, p_3)$; ε^0, μ^0 — permeabilities of the free half-space V^-.

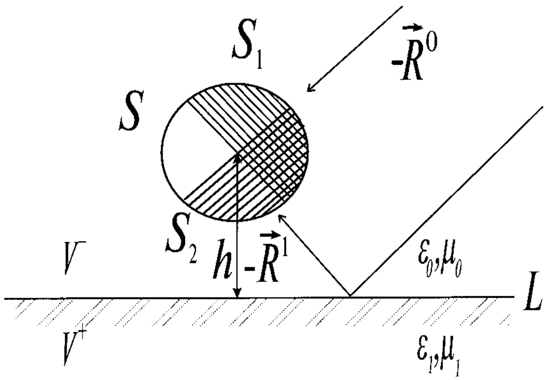

Figure 1. Geometry of scattering by perfectly conducting object with surface $\boldsymbol{S}$ located above the boundary of half-space $\boldsymbol{L}$.

In some cases (for particular shape of the surface $\boldsymbol{S}$ and mutual configuration of the surface $\boldsymbol{S}$ and the plane $\boldsymbol{L}$), one can neglect multiple re-reflections between the object and underlying surface as a second-order effects (in comparison with single reflection from $\boldsymbol{L}$ plane). This is a precisely "nonresonant" situation which will be considered in the paper.

So, we believe that surface $\boldsymbol{S}$ is illuminated by the plane wave (1) and by the wave one time reflected from $\boldsymbol{L}$ plane. First, we must obtain integral representations for fields scattered by such system.

Let $\vec{\boldsymbol{\mathcal{E}}}(x|x_0,\vec{p})$, $\vec{\boldsymbol{\mathcal{H}}}(x|x_0,\vec{p})$ be a field, generated by point dipole located in x_0 point with $\vec{p}$ vector-moment in the presence of half-space V^+. $\vec{\boldsymbol{\mathcal{E}}}(x|x_0,\vec{p})$, $\vec{\boldsymbol{\mathcal{H}}}(x|x_0,\vec{p})$ field obeys Maxwell's equations

$$\begin{cases} \operatorname{rot}\vec{\boldsymbol{\mathcal{E}}} = j\omega\mu_0\vec{\boldsymbol{\mathcal{H}}} \\ \operatorname{rot}\vec{\boldsymbol{\mathcal{H}}} = -j\omega\varepsilon\vec{\boldsymbol{\mathcal{E}}} - j\omega\vec{p}\delta(x-x_0) \end{cases}, \tag{2}$$

where $\varepsilon = \begin{cases} \varepsilon_0, & x_0 \in V^- \\ \varepsilon_1, & x_0 \in V^+ \end{cases}.$

Notice that if the main part of sounding signal spectrum is above 50 MHz, it is possible to neglect the dispersive properties of absorbing medium with ground parameters [2].

The system of equations (2) is added by boundary conditions at media interface $\boldsymbol{L}$:

$$\vec{\boldsymbol{\mathcal{E}}}_T^+ = \vec{\boldsymbol{\mathcal{E}}}_T^-; \qquad \vec{\boldsymbol{\mathcal{H}}}_T^+ = \vec{\boldsymbol{\mathcal{H}}}_T^-. \tag{3}$$

Here and further $\vec{A}_T = \vec{A} - \vec{n}\left(\vec{A}\vec{n}\right)$, $\vec{B}_\perp = \left(\vec{n} \times \vec{B}\right)$, $\vec{n}$ is a unit vector of normal to corresponding boundary.

Consider field $\vec{E}(\vec{x})$, $\vec{H}(\vec{x})$ generated by the given distribution of current volume density $\vec{J}$ in the region V^- in the presence of half-space V^+ and perfectly conducting scatterer $\boldsymbol{S}$. For this case Maxwell's equations are:

$$\begin{cases} \operatorname{rot} \vec{E} = j\omega\mu_0 \vec{H} \\ \operatorname{rot} \vec{H} = -j\omega\varepsilon \vec{E} + \vec{J} \end{cases} \tag{4}$$

Notice that $\partial V^- = L \cup S$ is boundary of the region V^- (Fig. 1). Boundary conditions at media interface $\boldsymbol{L}$

$$\vec{E}_T^+ = \vec{E}_T^-; \qquad \vec{H}_T^+ = \vec{H}_T^-. \tag{5}$$

should be added by requirement at the surface $\boldsymbol{S}$:

$$\vec{E}_T|_S = 0. \tag{6}$$

Lorenz's lemma for fields $(\vec{E}(\vec{x}), \vec{H}(\vec{x}))$ and $(\vec{\boldsymbol{\mathcal{E}}}(x|x_0,\vec{p}), \vec{\boldsymbol{\mathcal{H}}}(x|x_0,\vec{p}))$ in the region V^- provided $x_0 \in V^-$ yields:

$$\int_L \left(\vec{E}_T^- \cdot \vec{\boldsymbol{\mathcal{H}}}_\perp^- - \vec{\boldsymbol{\mathcal{E}}}_T^- \cdot \vec{H}_\perp^-\right) dl - \int_S \vec{\boldsymbol{\mathcal{E}}}_T^- \cdot \vec{H}_\perp^- ds \\ = -\int_{V^-} \left(j\omega\vec{p}\delta(x-x_0)\vec{E} + \vec{J} \cdot \vec{\boldsymbol{\mathcal{E}}}\right) dv. \tag{7}$$

Using filtering properties of δ-function and superposition principle, we obtain the representation:

$$j\omega\vec{p}\left(\vec{E}(x_0) - \vec{\boldsymbol{\mathcal{E}}}(x_0)\right) \\ = \int_S \vec{\boldsymbol{\mathcal{E}}}_T(x|x_0,\vec{p}) \cdot \vec{H}_\perp(x) ds - \int_L \left(\vec{E}_T^- \cdot \vec{\boldsymbol{\mathcal{H}}}_\perp^- - \vec{\boldsymbol{\mathcal{E}}}_T^- \cdot \vec{H}_\perp^-\right) dl, \tag{8}$$

where $\vec{\boldsymbol{\mathcal{E}}}(x_0)$ is a field generated by the given distribution of extrinsic currents $\vec{J}$ in half-space V^- without scatterer $\boldsymbol{S}$.

By applying Lorenz's lemma to the same fields in the region V^+, we obtain

$$0 = \int\limits_L \left(\vec{E}_T^+ \cdot \vec{\boldsymbol{\mathcal{H}}}_\perp^+ - \vec{\boldsymbol{\mathcal{E}}}_T^+ \cdot \vec{H}_\perp^+ \right) dl. \tag{9}$$

Adding relations (8) and (9), term by term, and accounting for boundary conditions (3), (5), (6), it is possible to obtain the following integral representation for field $\vec{E}(x_0)$:

$$j\omega\vec{p}\left(\vec{E}(x_0) - \vec{\boldsymbol{\mathcal{E}}}(x_0)\right) = \int\limits_S \vec{\boldsymbol{\mathcal{E}}}(x|x_0, \vec{p}) \cdot \vec{H}_\perp(x) ds. \tag{10}$$

Let $\vec{x}_0$ be a vector with length x_0 directed to radiation source

$$\vec{x}_0 = x_0 \vec{R}^0, \tag{11}$$

where $\vec{R}^0$ is unit vector.

Let $x_0 \to \infty$ in formula (10). As a result, representation (10) becomes:

$$j\omega\vec{p}\left(\vec{E}\left(\vec{R}^0\right) - \vec{\boldsymbol{\mathcal{E}}}\left(\vec{R}^0\right)\right) = \int\limits_S \vec{\boldsymbol{\mathcal{E}}}_T\left(x|\vec{R}^0, \vec{p}\right) \cdot \vec{H}_\perp(x) ds. \tag{12}$$

Here $\vec{\boldsymbol{\mathcal{E}}}\left(x|\vec{R}^0, \vec{p}\right)$ is a field generated by the plane wave

$$\vec{\boldsymbol{\mathcal{E}}}_0\left(x|\vec{R}^0, \vec{p}\right) = k_0^2 \omega \sqrt{\frac{\mu_0}{\varepsilon_0}} \vec{p}^{\,0} \exp\left(-jk_0\left(\vec{R}^0 \cdot \vec{x}\right)\right) \cdot \Omega(k_0 x_0), \tag{13}$$

where $\Omega(k_0 x_0) = \frac{1}{4\pi} \frac{\exp(jk_0 x_0)}{k_0 x_0}$, propagating in direction $-\vec{R}^0$ in the presence of half-space V^+ only (without scatterer $\boldsymbol{S}$); $\vec{E}(\vec{R}^0)$, $\vec{\boldsymbol{\mathcal{E}}}(\vec{R}^0)$ are the back scattered fields (in far zone) when scatterer $\boldsymbol{S}$ is present and scatterer $\boldsymbol{S}$ is absent, respectively.

The plane wave (13) occurred by passing to the limit in vector-function

$$\vec{\boldsymbol{\mathcal{E}}}(x|x_0, \vec{p}) = \frac{1}{\varepsilon_0}\left[\vec{\nabla}\left(\vec{p}\vec{\nabla}g\right) + k^2 \vec{p} g\right], \quad \left(g(x, x_0) = \frac{\exp(jk_0|\vec{x} - \vec{x}_0|)}{4\pi|\vec{x} - \vec{x}_0|}\right)$$

expressing field of the dipole located in free space at point $x_0 \in V^-$ which is removed to infinity. In doing so, the following asymptotic expansion of function $g(x, x_0)$ at $x_0 \to \infty$ has been used:

$$g(x, x_0) \sim k_0 \Omega (k_0 x_0) \exp\left(-jk_0 \left(\vec{R}^0 \cdot \vec{x}\right)\right)$$

In the general case, the plane wave (13) incidence on media interface $\boldsymbol{L}$ is obliquely. In this case, it is believed that field scattered in direction $\vec{R}^0$, is equal to zero $(\vec{\boldsymbol{\mathcal{E}}}\left(\vec{R}^0\right) = 0)$. Thus, expression for field above $\boldsymbol{L}$ (near $\boldsymbol{L}$) surface without scatterer $\boldsymbol{S}$ has the following form:

$$\vec{\boldsymbol{\mathcal{E}}}\left(x|\vec{R}^0, \vec{p}\right) = k_0^2 \omega \sqrt{\frac{\mu_0}{\varepsilon_0}} \left[\vec{p}^{\,0} \exp\left(-jk_0 \left(\vec{R}^0 \cdot \vec{x}\right)\right) + \right.$$
$$\left. + \vec{p}^1 \exp\left(-jk_0 \left(\vec{R}^1 \cdot \vec{x}\right)\right)\right] \Omega (k_0 x_0), \qquad (14)$$

where $-\vec{R}^1 = -\vec{R}^0 + 2\vec{n}\left(\vec{R}^0 \cdot \vec{n}\right)$ is a propagation direction of the wave reflected from surface $\boldsymbol{L}$, $\vec{p}^1$ is an unknown vector to be calculated, for example, by the method elaborated in [1].

The phase paths that are associated with reflection from boundary $\boldsymbol{L}$ must be taken into account. Let $\boldsymbol{M}$ be a point at the object surface with radius-vector $\vec{x}$ in some coordinate system $\boldsymbol{OX}_1\boldsymbol{X}_2\boldsymbol{X}_3$ and $\boldsymbol{C}$ be a point of a mirror reflection from plane $\boldsymbol{L}$. The reflected beam from point $\boldsymbol{C}$ passes through point $\boldsymbol{M}$ on $\boldsymbol{S}$ (Fig. 2).

The plane $\boldsymbol{L}$ is described by the equation

$$(\vec{x} \cdot \vec{n}) + h = 0, \qquad (15)$$

where h is a distance from plane $\boldsymbol{L}$ to the origin of the coordinate system along the normal vector $\vec{n}$ direction to plane $\boldsymbol{L}$.

Denote $\vec{c} = \vec{OC} = \vec{x} - \lambda \vec{R}^1$; $\vec{\xi} = \vec{CM} = \vec{x} - \vec{c} = \lambda \vec{R}^1$, where λ is determined from the condition that point $\boldsymbol{C}$ belong to plane $\boldsymbol{L}$:

$$\lambda = \frac{(\vec{x} \cdot \vec{n}) + h}{\left(\vec{R}^1 \cdot \vec{n}\right)}. \qquad (16)$$

So, incident wave (13) is represented in the form:

$$\vec{\boldsymbol{\mathcal{E}}}\left(x|\vec{R}^0, \vec{p}\right) = \Omega (k_0 x_0) k_0^2 \omega \sqrt{\frac{\mu_0}{\varepsilon_0}} \vec{p}^{\,0} \exp\left(-jk_0 \left(\vec{R}^0 \cdot \left(\vec{c} + \vec{\xi}\right)\right)\right)$$

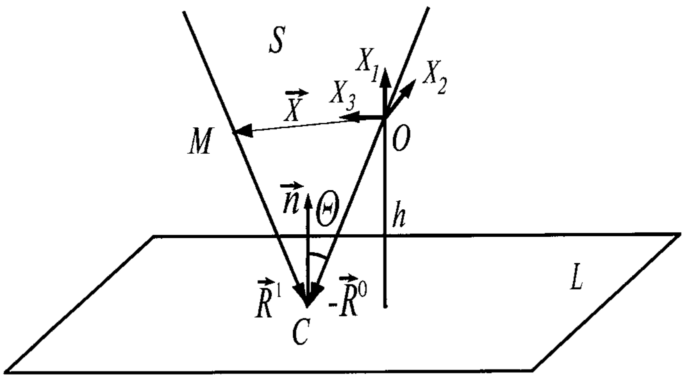

Figure 2. Calculation of the phase paths of the wave re-reflected from the media interface.

$$= \Omega\left(k_0 x_0\right) k_0^2 \omega \sqrt{\frac{\mu_0}{\varepsilon_0}} \vec{p}^{\,0} \exp\left(-jk_0\left(\vec{R}^0 \cdot \vec{c}\right)\right) \exp\left(-jk_0\left(\vec{R}^0 \cdot \vec{\xi}\right)\right)$$
$$= \hat{\vec{p}}^{\,0} \exp\left(-jk_0\left(\vec{R}^0 \cdot \vec{\xi}\right)\right),$$

and the reflected wave respectively in the form:

$$\vec{\boldsymbol{\mathcal{E}}}\left(x|\vec{R}^1, \vec{p}^1\right) = \hat{\vec{p}}^{\,1} \exp\left(-jk_0\left(\vec{R}^1 \cdot \vec{\xi}\right)\right)$$
$$= \Omega\left(k_0 x_0\right) k_0^2 \omega \sqrt{\frac{\mu_0}{\varepsilon_0}} \vec{p}^1 \exp\left(-jk_0\left(\vec{R}^0 \cdot \vec{c}\right)\right) \exp\left(-jk_0\left(\vec{R}^1 \cdot \vec{\xi}\right)\right)$$
$$= \Omega\left(k_0 x_0\right) k_0^2 \omega \sqrt{\frac{\mu_0}{\varepsilon_0}} \vec{p}^1 \exp\left(-jk_0\left(\left(\vec{R}^0 - \vec{R}^1\right) \cdot \vec{c} + \vec{R}^1 \cdot \vec{x}\right)\right).$$

Thus, the summary field at the point $\vec{x}$ at surface of the object $\boldsymbol{S}$, taking into account phase paths, caused by original wave reflection from plane $\boldsymbol{L}$, may be written:

$$\vec{\boldsymbol{\mathcal{E}}}\left(x|\vec{R}^0, \vec{p}\right) = k_0^2 \omega \sqrt{\frac{\mu_0}{\varepsilon_0}} \left[\vec{p}^{\,0} \exp\left(-jk_0\left(\vec{R}^0 \cdot \vec{x}\right)\right)\right.$$
$$\left. + \vec{p}^1 \exp\left(-jk_0\left(\left(\vec{R}^0 - \vec{R}^1\right) \cdot \vec{c} + \vec{R}^1 \cdot \vec{x}\right)\right)\right] \times \Omega\left(k_0 x_0\right). \quad (17)$$

Considering (17) we obtain from (12):

$$\vec{p}\vec{E}\left(\vec{R}^0\right) = -j\Omega\left(k_0 x_0\right) k_0^2 \sqrt{\frac{\mu_0}{\varepsilon_0}} \times \int_S \left[\vec{p}^{\,0} \exp\left(-jk_0\left(\vec{R}^0 \cdot \vec{x}\right)\right)\right.$$

$$+\vec{p}^1\exp\left(-jk_0\left(\left(\vec{R}^0-\vec{R}^1\right)\cdot\vec{c}+\vec{R}^1\cdot\vec{x}\right)\right)\Big]\,\vec{H}_\perp(\vec{x})\,ds. \quad (18)$$

Notice, that $\vec{H}_\perp(\vec{x})$ is a surface current density on $\boldsymbol{S}$, generated by the plane wave propagating in the direction $-\vec{R}^0$ in the presence of boundary $\boldsymbol{L}$ of half-space V^+. The presence of half-space V^+ in considered system results in additional wave (reflected from plane L and propagating in direction $-\vec{R}^1$) incidence on surface S. So, two mutually intersecting (in general case) "illuminated" regions S_1 and S_2 are localized on the surface of the object (Fig. 1). Then, in physical optics approximation, a surface current density in the region $\boldsymbol{S}$ can be expressed in the form:

$$\vec{H}_\perp(\vec{x}) = \begin{cases} 2\vec{n}\times\vec{H}_1^0, & \vec{x}\in S_1, \\ 2\vec{n}\times\vec{H}_2^0, & \vec{x}\in S_2, \end{cases} \quad (19)$$

where

$$\begin{aligned} \vec{H}_1^0 &= \left(\vec{p}^{\,0}\times\vec{R}^0\right)\sqrt{\frac{\varepsilon_0}{\mu_0}}\exp\left(-jk_0\left(\vec{R}^0\cdot\vec{x}\right)\right), \\ \vec{H}_2^0 &= \left(\vec{p}^1\times\vec{R}^1\right)\sqrt{\frac{\varepsilon_0}{\mu_0}}\exp\left(-jk_0\left(\vec{R}^0-\vec{R}^1\right)\cdot\vec{c}\right)\exp\left(-jk_0\left(\vec{R}^1\cdot\vec{x}\right)\right). \end{aligned} \quad (20)$$

From the preceding, the expression (18) can be transformed into a sum of two surface integrals:

$$\begin{aligned} \vec{p}\cdot\vec{E}\left(\vec{R}^0\right) = &-jk_0\times\Bigg\{\int_{S_1}\Big[A_0(\vec{x})\exp\left(-jk_0\left(2\vec{R}^0\cdot\vec{x}-r\right)\right) \\ &+A_1(\vec{x})\exp\left(-jk_0\left(\left(\vec{R}^0+\vec{R}^1\right)\cdot\vec{x}+\left(\vec{R}^0-\vec{R}^1\right)\cdot\vec{c}-r\right)\right)\Big]\,ds \\ &+\int_{S_2}\Big[B_0(\vec{x})\exp\left(-jk_0\left(2\left(\vec{R}^1\cdot\vec{x}+\left(\vec{R}^0-\vec{R}^1\right)\cdot\vec{c}\right)-r\right)\right) \\ &+B_1(\vec{x})\exp\left(-jk_0\left(\left(\vec{R}^0+\vec{R}^1\right)\cdot\vec{x}+\left(\vec{R}^0-\vec{R}^1\right)\cdot\vec{c}-r\right)\right)\Big]\,ds\Bigg\}, \end{aligned} \quad (21)$$

where $r = x_0$ is a distance from the radiation source to the object;

$$A_0(\vec{x}) = \frac{1}{2\pi r}\left(\vec{R}^0\cdot\vec{n}\right),$$

$$A_1(\vec{x}) = \frac{1}{2\pi r}\left(\left(\vec{p}^{\,0}\cdot\vec{p}^{1}\right)\cdot\left(\vec{R}^0\cdot\vec{n}\right) - \left(\vec{p}^{1}\cdot\vec{R}^0\right)\cdot\left(\vec{p}^{\,0}\cdot\vec{n}\right)\right),$$
$$B_0(\vec{x}) = \frac{1}{2\pi r}\left(\vec{R}^1\cdot\vec{n}\right)\left|\vec{p}^{1}\right|^2,$$
$$B_1(\vec{x}) = \frac{1}{2\pi r}\left(\left(\vec{p}^{\,0}\cdot\vec{p}^{1}\right)\cdot\left(\vec{R}^1\cdot\vec{n}\right) - \left(\vec{p}^{\,0}\cdot\vec{R}^1\right)\cdot\left(\vec{p}^{1}\cdot\vec{n}\right)\right).$$

Using the connection between short-wave asymptotics of scattered wave and asymptotic behavior of transient response $\vec{\mathcal{E}}(t)$ near the wave front one can obtain:

$$\begin{aligned}\vec{p}\cdot\vec{\boldsymbol{\mathcal{E}}}(t) = \frac{\partial}{\partial t}\Bigg\{\int\limits_{S_1}\Big[&A_0(\vec{x})\,\delta\left(t+2\left(\vec{R}^0\cdot\vec{x}\right)-r\right)\\ &+A_1(\vec{x})\,\delta\left(t+\left(\vec{R}^0+\vec{R}^1\right)\cdot\vec{x}+\left(\vec{R}^0-\vec{R}^1\right)\cdot\vec{c}-r\right)\Big]\,ds\\ &+\int\limits_{S_2}\Big[B_0(\vec{x})\,\delta\left(t+2\left(\left(\vec{R}^0-\vec{R}^1\right)\cdot\vec{c}+\vec{R}^1\cdot\vec{x}\right)-r\right)\\ &+B_1(\vec{x})\,\delta\left(t+\left(\vec{R}^0+\vec{R}^1\right)\cdot\vec{x}+\left(\vec{R}^0-\vec{R}^1\right)\cdot\vec{c}-r\right)\Big]\,ds\Bigg\}. \qquad (22)\end{aligned}$$

Taking into account

$$\left(\vec{R}^0-\vec{R}^1\right)\cdot\vec{c} = 2\vec{n}\cos\theta\vec{x} - 2\left(\vec{x}\cdot\vec{n}\right)\cos\theta - 2h\cos\theta = -2h\cos\theta, \quad (23)$$

expression (22) is transformed to the form:

$$\begin{aligned}\vec{p}\cdot\vec{\boldsymbol{\mathcal{E}}}(t) = \frac{\partial}{\partial t}\Bigg\{\int\limits_{S_1}\Big[&A_0(\vec{x})\,\delta\left(t+2\left(\vec{R}^0\cdot\vec{x}\right)-r\right)\\ &+A_1(\vec{x})\,\delta\left(t+\left(\vec{R}^0+\vec{R}^1\right)\cdot\vec{x}-(2h\cos\theta)-r\right)\Big]\,ds\\ &+\int\limits_{S_2}\Big[B_0(\vec{x})\,\delta\left(t+2\left(\vec{R}^1\cdot\vec{x}\right)-(4h\cos\theta)-r\right)\\ &+B_1(\vec{x})\,\delta\left(t+\left(\vec{R}^0+\vec{R}^1\right)\cdot\vec{x}-(2h\cos\theta)-r\right)\Big]\,ds\Bigg\}. \qquad (24)\end{aligned}$$

Note that the integrals in (24) look like ones in [1] structurally. Using a relation between impulse characteristic $\vec{\boldsymbol{\mathcal{E}}}(t)$ and transient characteristic $\hat{\vec{\boldsymbol{\mathcal{E}}}}(t)$ (response to step-function):

$$\hat{\vec{\boldsymbol{\mathcal{E}}}}(t) = \int \vec{\boldsymbol{\mathcal{E}}}(t)dt, \tag{25}$$

and, reasoning by analogy with [1], we obtain a final expression for a projection of transient characteristic at arbitrary direction $\vec{p}$:

$$\vec{p} \cdot \hat{\vec{\boldsymbol{\mathcal{E}}}}(t) = \int\limits_{\Gamma_{11}(t)} \frac{A_0(\vec{x})}{\sqrt{1-\left(\vec{R}^0 \cdot \vec{n}\right)^2}} dl + \int\limits_{\Gamma_{12}(t)} \frac{A_1(\vec{x})}{\sqrt{1-\left(\frac{\left(\vec{R}^0+\vec{R}^1\right)\cdot\vec{n}}{\left|\vec{R}^0+\vec{R}^1\right|}\right)^2}} dl$$
$$+ \int\limits_{\Gamma_{21}(t)} \frac{B_0(\vec{x})}{\sqrt{1-\left(\vec{R}^1 \cdot \vec{n}\right)^2}} dl + \int\limits_{\Gamma_{22}(t)} \frac{B_1(\vec{x})}{\sqrt{1-\left(\frac{\left(\vec{R}^0+\vec{R}^1\right)\cdot\vec{n}}{\left|\vec{R}^0+\vec{R}^1\right|}\right)^2}} dl \tag{26}$$

where integral contours $\Gamma_{ij}(t)$ are intersections of "illuminated" regions S_1, S_2 with planes determinated by different combinations of vectors $\vec{R}^0$ and $\vec{R}^1$:

$$\Gamma_{11}(t) : \{S_1 \cap \Pi_1\}, \qquad \Gamma_{12}(t) : \{S_1 \cap \Pi_2\},$$
$$\Gamma_{21}(t) : \{S_2 \cap \Pi_3\}, \qquad \Gamma_{22}(t) : \{S_2 \cap \Pi_4\},$$

$\Pi_i (i = 1, \ldots, 4)$ are planes given by the equations

$$-2\vec{R}^0 \cdot \vec{x} + r = t \qquad (\Pi_1);$$
$$-\left(\vec{R}^0 + \vec{R}^1\right) \cdot \vec{x} + 2h\cos\theta + r = t \qquad (\Pi_2);$$
$$-2\vec{R}^1 \cdot \vec{x} + 4h\cos\theta + r = t \qquad (\Pi_3);$$
$$-\left(\vec{R}^0 + \vec{R}^1\right) \cdot \vec{x} + 2h\cos\theta + r = t \qquad (\Pi_4);$$

and θ is an incident angle of a plane wave (with respect to boundary $\boldsymbol{L}$). Thus, transient characteristic calculation is reduced to computation of four contour integrals.

Obtaining (26) from relations (24) and (25) is based on formal passing to the limit in finite-difference ratio for calculation of derivatives with respect to t.

Comparison of obtained expression for the transient characteristic with the integral describing bistatic transient characteristic of a single object [1] allows to conclude that each integral in expression (26) for transient characteristic can be interpretated in terms of bistatic scattering problem solution. The contribution of the first integral to a transient characteristic is caused by direct reflection of original plane wave from surface $\boldsymbol{S}$ (without accounting for re-reflections from plane $\boldsymbol{L}$); the rest integrals contribute to transient characteristic from other possible combinations of "illuminated" regions with directions of wave interacting with surface $\boldsymbol{S}$ and plane $\boldsymbol{L}$.

We can obtain an expression of transient response for arbitrary pulse excitation using transient characteristic $\hat{\vec{\boldsymbol{\mathcal{E}}}}(t)$ of system and expression for sounding signal $Q(t)$ of duration τ:

$$\vec{E}(t) = \int\limits_0^T Q'(s)\hat{\vec{\boldsymbol{\mathcal{E}}}}(t-s)ds, \tag{27}$$

where $T = \min\{\tau, t\}$.

3. NUMERICAL RESULTS

Samples of numerical results are presented in this section in order to validate the proposed technique.

Perfectly conducting sphere of radius 1 m, generalized models of a real tank and B-2 aircraft are taken as an object of research. All objects are placed over half-space with different ground parameters.

For numerical calculations, a mathematical models of ultrawideband and radiopulse sounding signals were chosen in the form respectively:

$$Q(t) = \frac{1}{\sqrt{\pi\tau}} \exp\left[-\frac{t^2}{\tau^2}\right] - \frac{1}{1.5\sqrt{\pi\tau}} \exp\left[-\frac{t^2}{1.5\tau^2}\right], \tag{28}$$

$$Q(t) = \frac{1}{\sqrt{\pi\tau}} \exp\left[-\frac{t^2}{\tau^2}\right] \cos(k_0 t), \tag{29}$$

where τ is a pulse duration in "light" meters ($\tau = c\tau_1$, c is speed of light, τ_1 is pulse duration). Duration τ_1 of sounding signals is equal

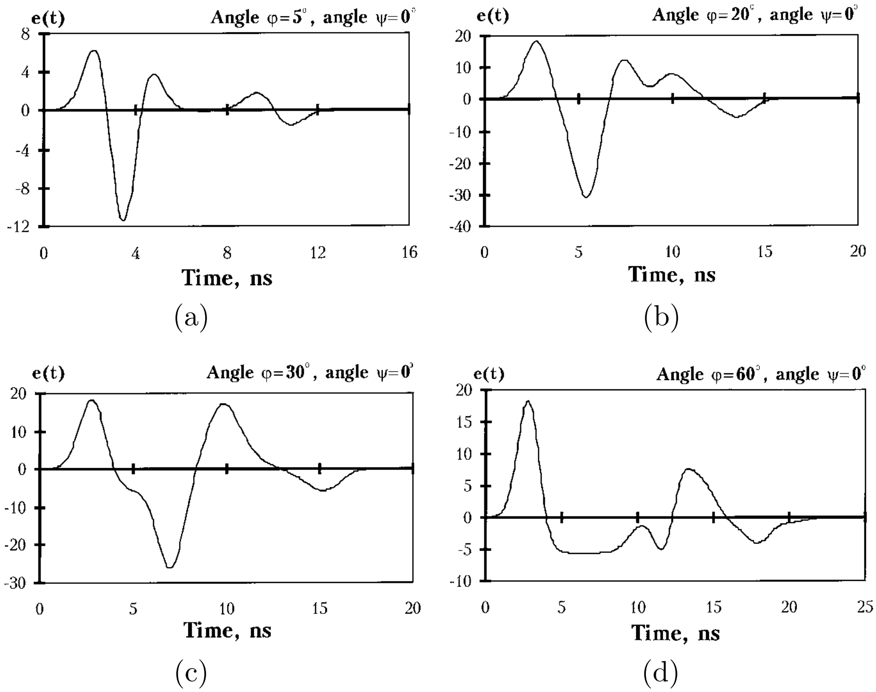

Figure 3. The ultrawideband response of the sphere of 1 m radius located at height 1 m above underlying surface.

to 1 ns. Notice that spectra of both signals occupy the high-frequency range that justifies using of high-frequency approximation for object transient characteristics. The number of temporal dependencies of normalized electric field $e(t)$ were obtained for different illumination angles and horizontal polarization of incident plane wave (Figs. 3, 4, 6, 8). The uniform half-space has the following parameters: relative dielectric permeability—$\varepsilon = 7$ and relative magnetic permeability—$\mu = 1$, $\sigma = 10^{-3}$ Sm/m. The origin of coordinate system is placed in the center of the object. Angles φ and ψ of spherical coordinate system determine direction of the illumination (unit vector $\vec{R}^0$). The angle φ is counted from the positive direction of axis OX_3 in plane OX_1X_3 and is changed clockwise from $0°$ to $180°$, while the zero value of angle ψ is on axis OX_3 and the angle ψ is counted clockwise in a plane which is parallel to dielectric half-space (Fig. 2).

In Figures 3 and 4, sphere responses to ultrawideband pulse of duration $\tau_1 = 1$ ns and radiopulse with the same duration and carrier

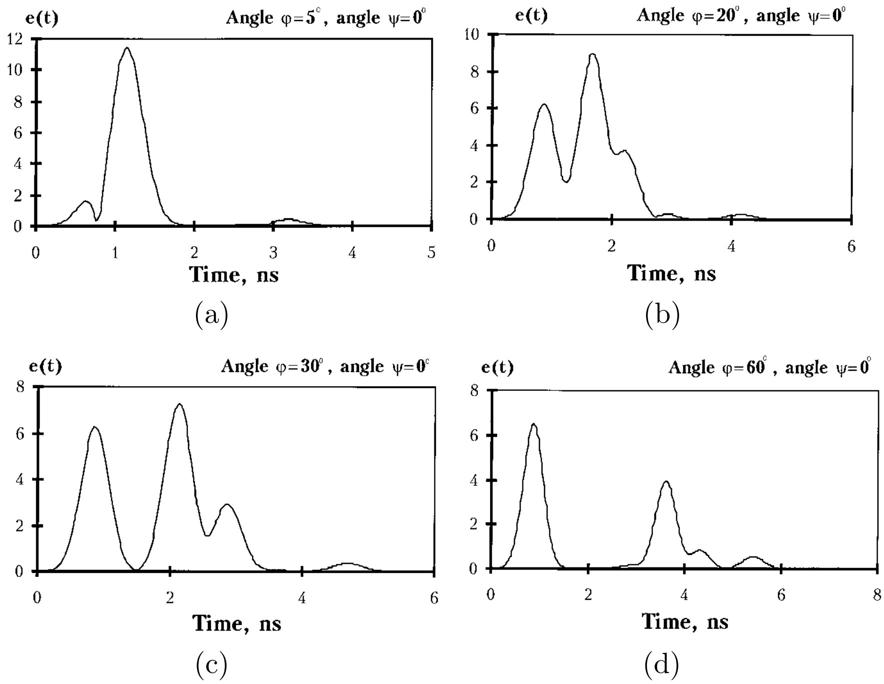

Figure 4. The radiopulse response of the sphere of 1 m radius located at height 1 m above underlying surface.

frequency of 10 GHz, respectively, are plotted for different angles φ and $\psi = 0°$. The center of the sphere is placed at a height $h = 1$ m over the dielectric half-space (sphere and matter have a contact point).

For ultrawideband pulses, when angle φ is near to $0°$, we obtain positive partial pulses of small amplitude and rather big negative ones (Fig. 3a). An increase of angle φ accompanies an appearance of the second positive pulse (for example, if $\varphi = 30°$ the second pulse is noticeable obviously (Fig. 3c)), a reduction of negative part and isolation of a signal response from the sphere in a free space (Fig. 3d) are observed. In addition, an increase of angle φ results in decreasing of the second partial pulse which is determined by re-reflections between material half-space and "illuminated" region S_2.

As one can see from Fig. 4, the radiopulse response (signal envelope) presents some pulses from "bright" points located at different "illuminated" regions of the object. When angle φ is near $0°$ a separation of pulses from different "bright" points is impossible (Fig. 4a), which results in the large response amplitude. On increase of angle φ

the partial pulses from each "bright" point are observed clearly. Furthermore, we can see a reduction of the amplitude of pulses caused by the re-reflections from material half-space (Fig. 4d), as in the case of ultrawideband sounding pulse.

Furthermore, this method allows to calculate an electromagnetic pulse scattering from complex shape objects. As an example, response calculation results have been considered for a single (without matter half-space influence) generalized tank model and for a model of a tank which is placed on dry ground.

The ellipsoid surface parts are used to describe a surface of a tank model. The surface approximation method for a complex shape object has been considered in [1]. In Fig. 5, an approximated surface of the tank is present. Determination of "illuminated" region for such complex object as a tank is based the routing algorithm from [3].

In Fig. 6 a single tank and tank on dry ground responses to ultrawideband pulse (Fig. 6a, 6b) and to radiopulse (Fig. 6c, 6d) are shown for $\varphi = 30^\circ$ and $\psi = 0^\circ$. For ultrawideband sounding the influence of the material half-space manifests itself as an increase of a partial pulse amplitudes and appearance of additional pulses (Fig. 6b). For radiopulse sounding amplitude of a response of the tank on dry ground (Fig. 6d) increases (in contrast to a response of a single object (Fig. 6c)) and response is also getting more smoothed.

Besides, the calculations of the responses of the perfectly conducting model B-2 aircraft was carried out. The approximation of this model surface is presented in Fig. 7.

In Fig. 8 the responses of the single aircraft model (Fig. 8a, 8c) and the aircraft on the take-off strip (Fig. 8b, 8d), illuminated by ultrawideband and radiopulse signals at $\varphi = 30^\circ$ and $\psi = 0^\circ$ is presented.

The response of the aircraft has the more complicated shape and differs essentially from the response of the tank.

The analysis shows that such components of the aircraft as crew cabin and fuselage make the main contribution to the aircraft response. One can see that underlying surface also makes significant contribution to the aircraft response.

Notice, the suggested approximate method of the pulse backscattering calculation for perfectly objects near media interface can be used effectively, when object sizes are much more than sounding pulse duration (in "light" meters).

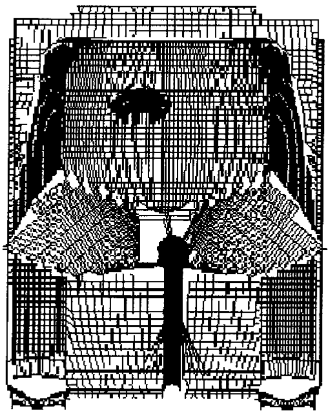

Figure 5. Generalized model of the tank. Elevation angle is 20 degrees, azimuth is 0 degrees.

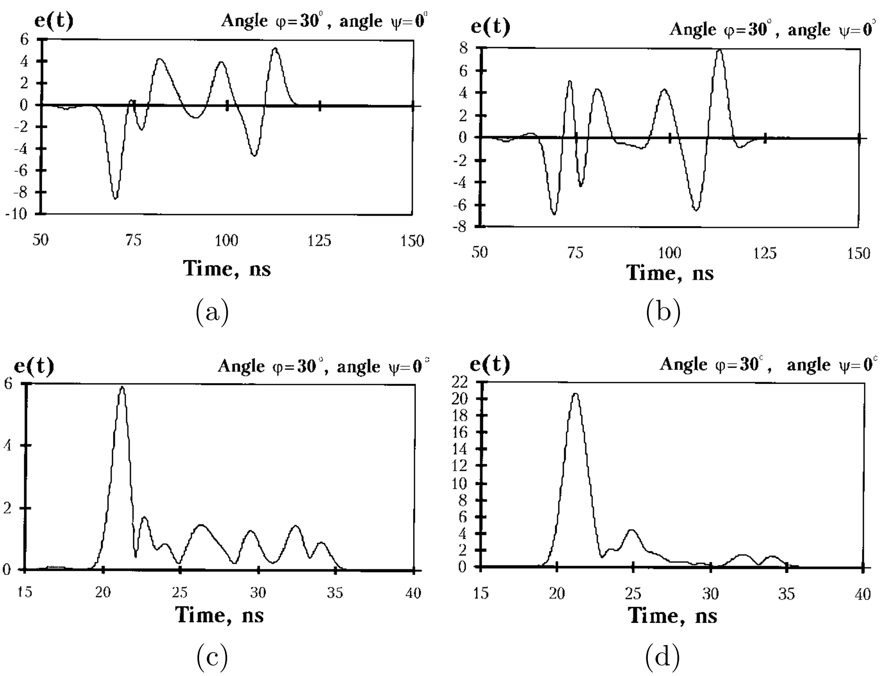

Figure 6. The pulse response of the tank (a. ultrawideband response of the tank in free space; b. ultrawideband response of the tank located on dry ground; c. radiopulse response of the tank in free space; d. radiopulse response of the tank located on dry ground).

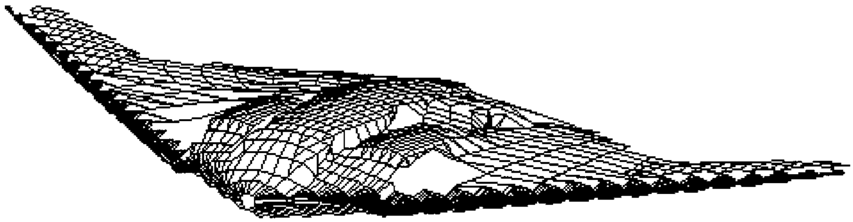

Figure 7. Generalized model of the B-2 aircraft. Elevation angle is 20 degrees, azimuth is 0 degrees.

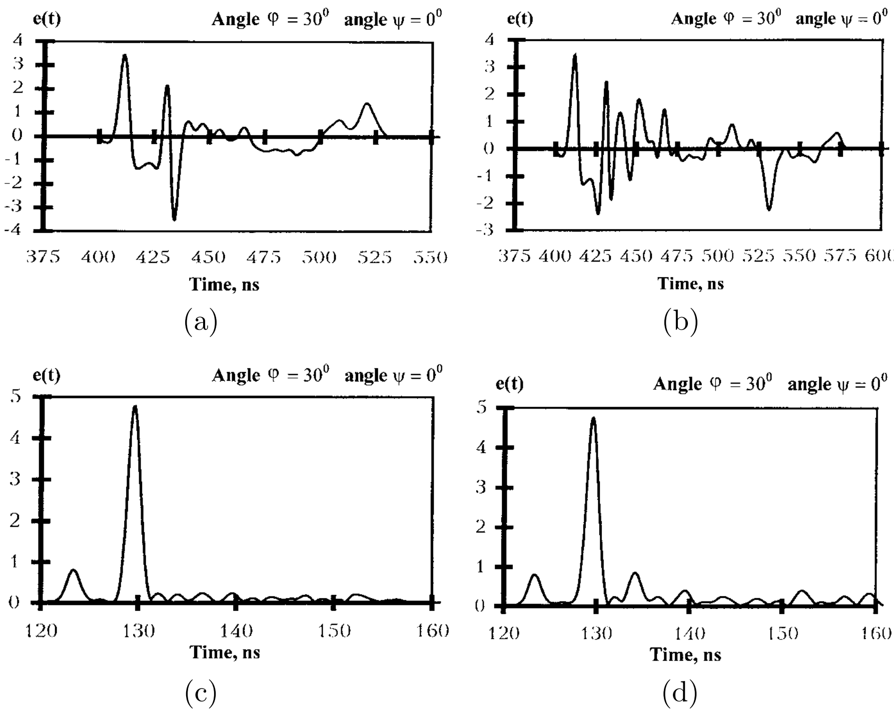

Figure 8. The pulse response of the B-2 aircraft (a. ultrawideband response of the B-2 aircraft in free space; b. ultrawideband response of the aircraft on the take-off strip; c. radiopulse response of the B-2 aircraft in free space; d. radiopulse response of the aircraft on the take-off strip).

4. CONCLUSION

In this paper, the scattering calculation method was applied to the pulse response analysis of the perfectly conducting electrically large object (with small curvatures) located near the boundary of the uniform half-space. This method may be used for calculation of complex shape objects' pulse responses.

REFERENCES

1. Sukharevsky, O. I., and V. A. Vasilets, "Impulse characteristic of smooth object in bystatic case," *Journal of Electromagnetic Wave and Applications,* Vol. 10, 1613–1622, 1996.
2. King, R., and G. Smith, *Antennas in Matter, Fundamentals Theory and Applications,* The MIT Press, Cambridge, Massachusetts and London, England, 1981.
3. Rodgers, D. F., *Procedural Elements for Computer Graphics,* McGraw-Hill Book Company, New York St. Lonis San Francisco, 1985.
4. Ufimtsev, P. Y., "Method of edge waves in the physical theory of diffraction," *Soviet Radio,* Moscow, 1962. Translated by U. S. Air Force, Foreign Technol. Div. Wright-Patterson AFB. OH. 1971: Tech. Rep. AD No. 733203 DTIC. Cameron Station, Alexandria, VA 22304-6145.